energies

MDPI

Article

Complementing Syngas with Natural Gas in Spark Ignition Engines for Power Production: Effects on Emissions and Combustion

Carlo Caligiuri [1,2,*], Urban Žvar Baškovič [3], Massimiliano Renzi [1], Tine Seljak [3], Samuel Rodman Oprešnik [3], Marco Baratieri [1] and Tomaž Katrašnik [3]

1 Faculty of Science and Technology, Free University of Bozen/Bolzano, 39100 Bolzano, Italy; massimiliano.renzi@unibz.it (M.R.); Marco.Baratieri@unibz.it (M.B.)
2 Institute for Applied Physics "Nello Carrara" (IFAC), Consiglio Nazionale delle Ricerche (CNR), Sesto Fiorentino, 50019 Firenze, Italy
3 Laboratory for Internal Combustion Engines and Electromobility, Faculty of Mechanical Engineering, University of Ljubljana, Aškerčeva 6, SI-1000 Ljubljana, Slovenia; urban.zvar-baskovic@fs.uni-lj.si (U.Ž.B.); tine.seljak@fs.uni-lj.si (T.S.); Samuel.RodmanOpresnik@fs.uni-lj.si (S.R.O.); tomaz.katrasnik@fs.uni-lj.si (T.K.)
* Correspondence: c.caligiuri@ifac.cnr.it

Abstract: Power generation units based on the bio-syngas system face two main challenges due to (i) the possible temporary shortage of primary sources and (ii) the engine power derating associated with the use of low-energy density fuels in combustion engines. In both cases, an external input fuel is provided. Hence, complementing syngas with traditional fuels, like natural gas, becomes a necessity. In this work, an experimental methodology is proposed, aiming at the quantification of the impact of the use of both natural gas and syngas in spark ignition (SI) engines on performance and emissions. The main research questions focus on investigating brake thermal efficiency (BTE), power derating, and pollutant emission (NO_x, CO, THC, CO_2) formation, offering quantitative findings that present the basis for engine optimization procedures. Experimental measurements were performed on a Toyota 4Y-E engine (a 4-cylinders, 4-stroke spark ignition engine) at partial load (10 kW) under different syngas energy shares (SES) and at four different spark ignition timings (10°, 25°, 35° and 45° BTDC). Results reveal that the impact of the different fuel mixtures on BTE is negligible if compared to the influence of spark advance variation on BTE. On the other hand, power derating has proven to be a limiting factor and becomes more prominent with increasing SES. An increasing SES also resulted in an increase of CO and CO_2 emissions, while NO_x and THC emissions decreased with increasing SES.

Keywords: spark ignition engines; renewable fuels; combustion; syngas; natural gas

Citation: Caligiuri, C.; Žvar Baškovič, U.; Renzi, M.; Seljak, T.; Oprešnik, S.R.; Baratieri, M.; Katrašnik, T. Complementing Syngas with Natural Gas in Spark Ignition Engines for Power Production: Effects on Emissions and Combustion. *Energies* **2021**, *14*, 3688. https://doi.org/10.3390/en14123688

Academic Editor: Constantine D. Rakopoulos

Received: 26 May 2021
Accepted: 17 June 2021
Published: 21 June 2021

1. Introduction

The always growing needs of energy security and environmental protection are pushing researchers and technicians to investigate and study the possibilities of using renewable fuels in current internal combustion engines to substitute or supplement conventional fossil fuels. In such a framework, a growing interest in the use of gaseous fuels (natural gas, hydrogen, syngas) is gathering attention among the scientific community. spark ignition (SI) engines, in which combustion mechanism is promoted by the spark plug, are more suitable for the use of gaseous fuels; on the other hand, compression ignition (CI) engines, in which the start of combustion process is controlled by a fuel ignition event, can be fueled with gaseous fuels only if a proper combustion strategy—such as dual fuel mode—is adopted [1–3]. The proposed study aims at analyzing the effect of the use of two different gaseous fuels, natural gas (NG) and syngas, in SI engines on emissions and combustion. Therefore, the proposed work focuses its attention on a particular fueling strategy. The numerous different technical factors influencing combustion development

and that are related to the construction and the design of the chosen SI engine—such as the design of the combustion chamber, the influence of the compression ratio, or the choice of the materials [4]—will not be discussed. In particular, the study fits in the framework of the use and the optimization of renewable energy sources for energy production, as suggested by the ambitious targets of the European Green Deal [5] in terms of fossil fuel substitution. The study focuses on the minimization of power derating while preserving high efficiency at low emissions, which are the main knowledge gaps that the authors are investigating. Syngas composition has been chosen in order to replicate a typical forestry biomass producer gas [6–8], and a methane rich NG is a substitute for a real-world application of a biomethane. The experimental analysis aims at replicating critical conditions in a gasification-based power plant unit whenever complementing bio-methane with producer gas becomes a necessity. Such peculiar conditions may occur for different reasons (shortage of primary sources, peak power output demand) that will be later analyzed. A state-of-the-art analysis of the use of the chosen fuels in spark-ignition engines will be now provided.

1.1. Natural Gas in SI Engines

Natural Gas (NG) is the most established and diffused gaseous fuel and currently represents one of the main alternatives to conventional liquid fossil fuels such as gasoline and diesel. NG is a fossil fuel that can be either extracted from other fossil fuels (crude oil in oil fields or coal in coal beds) or can be found on its own [9]. Given its composition, the main properties of NG are very close to those of methane (CH_4) and can vary depending on its origin [10]. The use of natural gas in internal combustion engines requires some modification to the typical spark ignition engine set-up. Since NG is usually introduced through injectors into the intake manifold, high-pressure compressed natural gas tanks are used to replace the liquid-fuel tank of conventional energy systems, in addition to high-pressure fuel lines [1]. Modified fuel injectors or fuel induction systems are required, as a higher mass and volume flow rates are needed to overcome the low density of natural gas [1]. A lower volumetric efficiency has to be considered and, as a consequence, power derating has to be taken into account. On the other hand, the high lower heating value (LHV) and octane number allow for higher compression ratios and therefore, when used together with turbocharging and intercooling, an increase in thermal power and efficiency, with respect to naturally aspirated SI-engines fueled with gasoline, can be obtained, e.g., [1]. NG combustion in internal combustion engines produces lower levels of carbon monoxide (CO) and unburned hydrocarbons (HC) when compared to traditional SI-engines fueled with gasoline and CI-engines fueled with diesel [11]. Moreover, as natural gas-powered SI-engines produce low smoke and particulate matter levels, their contribution to smog formation is minimal compared to SI-engines fueled with gasoline and diesel-powered CI-engines: that is why NG is particularly attractive for urban buses and local transportation in densely populated areas [1,12]. However, the use of NG in SI engines still faces different limitations. When compared to gasoline, NG has a lower laminar flame velocity, narrow flammability limits, high ignition energy requirements, and higher self-ignition temperature, leading to possible incomplete combustion or misfire. Although NG features high potential for use in SI engines, it is a fossil fuel that will have to be phased out to meet future greenhouse gas emissions and biofuels targets.

1.2. Syngas in SI Engines

In the framework of alternative fuels, biomass plays a relevant role in the sustainable energy challenge. The conversion of biomass into energy, based on short rotation forestry and other energy crops, can indeed contribute significantly to the reduction of greenhouse gas (GHG) emissions and the problems related to climate change [13]. The use of thermochemical processes, such as the gasification of biomass [7], allows the production of a gaseous fuel known as syngas. When produced from renewable energy (as defined in the Renewable Energy Directive II, part A of the Annex IX [14]), it can be considered

as an advanced gaseous biofuel. Commonly defined as a mixture of combustible and non-combustible gases, the term syngas can be used to indicate different gaseous fuels: (i) the main output of the gasification process, consisting of a mixture of H_2, CO, CO_2, CH_4 and, N_2, usually also defined as producer gas; (ii) the artificially obtained replica of producer gas, realized in lab-scale using gas bottles; (iii) a mixture of only combustible gases, namely H_2, CO, and potentially CH_4. Hence, when dealing with syngas, the definition of gas composition plays a crucial role in avoiding any kind of ambiguity. The very first attempts in using syngas in internal combustion engines were reported during the beginning of the XX century, mainly for power generation. Two extended reports published by the FAO Forestry Department [15] and by Kaupp and Goss [16] describe facts regarding gasification and the use of syngas in combustion engines. In the late 1930s, different initiatives related to the use of producer gas started to spread. Biomass-derived fueled SI engines were parts of different plans for independence from imported oil and the acceleration of the agriculture mechanization. Not long after World War II, abundant and cheap supplies of gasoline, diesel oil, and natural gas marked a major transformation in the transportation and energy conversion sectors. Such technological revolution was also drastically reflected in the academic research done in this field. Gasification and small-scale gas production technologies in particular were mostly overseen technology during this time period. A renewed interest in gasification technology, especially in the use of syngas, has recently grown, mainly driven by the need for renewable energy sources and clean power conversion technologies. Spark ignition engines require very few modifications to be fueled with syngas: it is their main advantage, and it justifies their diffusion as gas fueled SI engines. However, several combustion-related critical aspects need to be taken into strong consideration when dealing with syngas. As reported in several research works and summed up by the review work of Hagos et al. [17], a reduction of the output torque is usually associated with the use of syngas in SI engines when compared to its fossil-based counterparts (NG and gasoline). Such a trend tends to increase with decreasing LHV. Moreover, according to Martinez et al. [18] the lower volumetric efficiency, due to the low volumetric energy content of syngas [19], also has to be addressed as one of the main causes for such power derating. When compared to NG, the presence of H_2 is one of the most critical aspects related to syngas combustion [6]. Due to the boost in flame velocity brought by H_2, the spark timing should be retarded in order to avoid the development of excessive cylinder pressure and to optimize engine efficiency [18]. On the other hand, the presence of N_2 and CO_2 plays a positive role in reducing the knock tendency of the engine, which allows the use of higher compression ratios [6,20]. According to Sridhar et al. [21], the maximum brake torque point can be achieved by simultaneously retarding spark timing and increasing the compression ratio. Therefore, the optimal engine management when fueled with syngas has to be deeply investigated, as it depends on the fuel composition [2,19,22] and the characteristics of the engine.

1.3. Motivations, Focus and Research Questions

A number of research studies [23–28] have focused their attention on the use of different types of natural gas-derived fuels. One of the most studied investigations deals with the enrichment of NG with a fast-burning fuel, such as hydrogen, aiming at extending the lean operation limitations of NG fueled SI engines thanks to the improvements in terms of laminar burning velocities (i.e., hydrogen has a laminar burning velocity seven times higher than NG) [25]. Regardless, the use of such kinds of mixtures seems to be hindered by many practical difficulties, which include large-scale hydrogen production, storage, and fueling infrastructures as well as undesired combustion instabilities [25] in engines. Hagos et al. [23,26] have instead focused their attention on the blending of syngas (H_2/CO) with methane. The objective of this type of fueling strategy is to ensure higher specific power output as a consequence of the increasing the share of CH_4, which has a lower calorific value (LHV) that is five to ten times higher than syngas [23]. However, the production of H_2/CO syngas is still limited, as the most common way to produce syngas

is to use the end results of the gasification process of solid primary sources, which are typically a mixture of H_2, CO, CO_2, CH_4 and N_2. Other experimental analyses on dual fuel engines include the investigation of overall engine noise [29]. Power generation units based on the gasification system face two main drawbacks, which are both related to the output gaseous fuel obtained from biomass gasification. In real applications, it may be the case that the shortage of primary sources could affect the homogeneity of the producer gas generation, both in terms of composition and mass flow rate. Assuming a constant intake gas composition, drops in gas mass flow rates at the gasifier outflow sensibly affect the engine output power rates. Therefore, whenever the available fuel flow rate does not meet the required one, an external input fuel that is typically realized through the direct injection of natural gas [30] is required. A second critical aspect is related to the engine power derating [31] associated with the use of low-energy density fuels in combustion engines. Syngas power derating in spark ignition engines is usually quantified at around 15–40% of the maximum output power [32]. Whenever the required load exceeds the effective engine power output, an external input fuel has to be provided [27]. Hence, complementing syngas mixture with natural gas becomes a necessity. Finally, syngas composition also drastically affects the energy conversion capabilities of the system. Indeed, gas composition depends on many parameters, such as pellet size or gasifier operating temperature [7,33,34].

As it has emerged from the literature review, different critical, not yet elaborated on, aspects arise when the use of syngas and mixtures of syngas and natural gas in spark ignition engines in particular are concerned. With an aim to fill these knowledge gaps, the proposed work focuses on a systematic experimental investigation with an objective to quantify the impact of the use of both natural gas and syngas in spark ignition (SI) engines on its performance and emissions, which provides the basis for elucidating causal interrelations between fuel properties, their blending, and engine parameters. In particular, the study focuses on the combustion, performance, and emissions characteristics of CNG mixed at different shares with syngas (mixture of H_2, CO, CO_2, CH_4, and N_2) under a partial load condition and at a fixed engine speed. Moreover, the influence of the ignition time (by means of spark advance control) is evaluated in order to set the basis for an optimization of the engine operating parameters in a range of various applications. Thus, the main research questions addressed through the proposed investigation aim to clarify (i) what is the effect of the dual fuel combustion of NG and syngas on brake thermal efficiency (BTE) under different spark advance configurations?; (ii) how much does brake power derate as a consequence of the use of different fuel mixtures with different primary energy contents?; (iii) how are pollutant emissions (NO_x, CO, THC, CO_2) affected by the use of different fueling strategies? The final aim is to provide a quantitative investigation to set the basis for engine optimization strategies with the goal to either increase BTE or engine power or decrease engine-out emissions.

2. Materials and Methods

2.1. Experimental Set-Up

The experimental set-up is based on a Toyota 4Y-E, a 4-cylinders, 4-stroke spark ignition engine. The main engine characteristics are shown in Table 1.

Table 1. Toyota 4Y-E technical data.

Technical Characteristic	Value/Type	Unit
Nr. Cylinders	4	-
Valves per cylinder	2	-
Displacement	2237	cm^3
Bore	91	Mm
Stroke	86	Mm
Compression ratio	8.8	-
Max. Power @2570 rpm	42	kW
Max Torque @2200 rpm	160	Nm
Cooling system	Counter-current, water-cooled	-
Ignition system	Electronic ignition with inductors	-

The supply of both natural gas and syngas was controlled by a stepping motor, which opens or closes the throttle valve upstream of the intake manifold. Fuel mixing with air was ensured using a venturi gas mixer that had been designed following the work of Danardono et al. [35]. Syngas was provided by the Slovenian company "Istrabenz Plini" (http://www.istrabenzplini.si/ (accessed on 21 June 2021)). Its composition (see Table 2) reflects one of a typical producer gas obtained by the gasification of forestry biomass. It was provided as a mixture of gases, stored in tanks. Commercial natural gas with this composition, presented in Table 3, has been used as a representative of methane-rich natural gas, which could be substituted with a biomethane.

Table 2. Composition of the used syngas.

Component	CO	CO_2	H_2	CH_4	N_2
Vol. Fraction [%]	19.59%	12.48%	14.99%	2.49%	50.35%

Table 3. Composition of the used natural gas.

Component	CH_4	C_2H_6	C_3H_8	C_4H_{10}	N_2
Vol. Fraction [%]	95.65%	2.45%	0.78%	0.11%	0.65%

The engine was connected to a Borghi&Saveri FE260 dynamometer. The crankshaft position was measured using a Kistler 2613B angle encoder, while an AVL GH12D piezoelectric pressure transducer coupled with a charge amplifier was used to monitor in-cylinder pressure. Engine-out emissions were measured with two mobile emission analyzers simultaneously to cover all relevant species. During offline analysis, intake air humidity was considered to determine wet engine-out emissions from the measured values according to a standardized procedure [36]. Detailed information about the set-up is provided in Figure 1 and in Table 4.

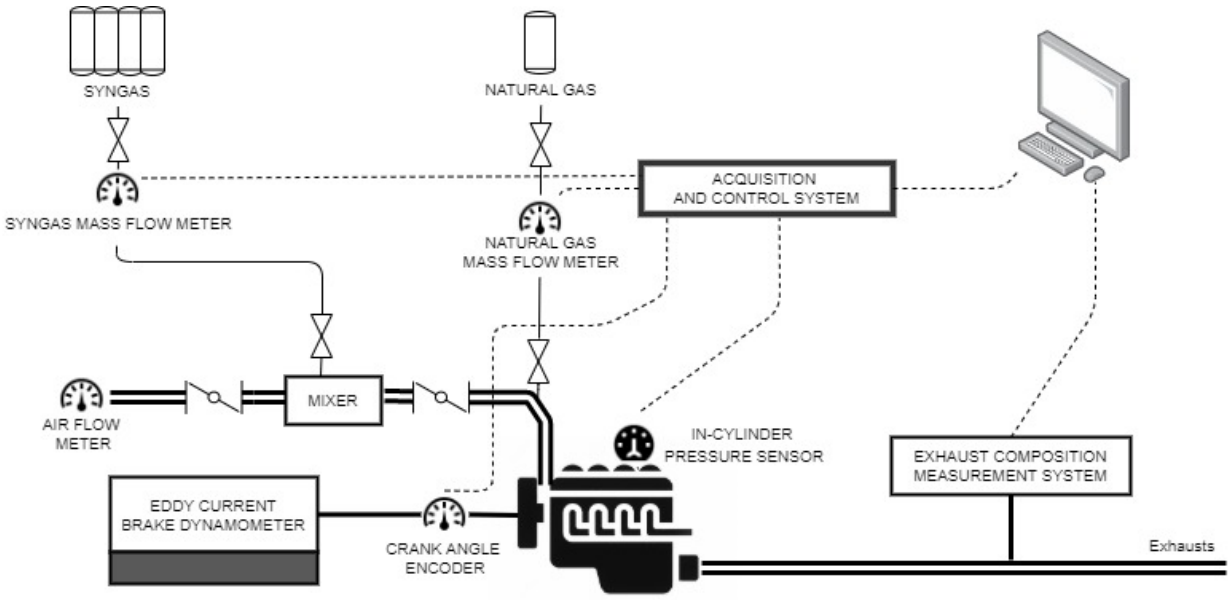

Figure 1. Scheme of the measurement system set-up.

Table 4. Measurement system information [1].

Measured Quantity	Equipment	Accuracy	Measuring Range
Air Mass Flow	Meriam 50MC2	±1% RD	0 to 100 SCFM
Syngas Mass Flow	Emerson Micromotion Elite CMFS015	±0.1% FS	0 to 330 kg/h
Natural Gas Mass Flow	Honeywell Elster RVG G10	±0.2% FS	0.5 to 16 m^3/h
Crank Angle	Kistler 2613B	±0.02 °CA at 10,000 rpm	1 to 20,000 rpm
In-cylinder pressure	AVL GH12D	±0.3% FS	0 to 300 bar
Torque	HBN U2B Load Cell	0.1% FS	0 to 2 kN
Exhausts composition: CO_2 and NO_x (NO and NO_2)	Sensors Semtech DS	<±2% RD <±2% RD <±2% RD	CO_2: 0 to 18% vol NO: 0 to 3000 ppm NO_2: 0 to 1000 ppm
Exhausts composition: CO and THC	Horiba OBS-2200	±2.5% RD ±2.5% RD	CO: 0 to 8% vol THC: 0 to 10,000 ppm

[1] Accuracy is expressed, according to the manufacturer provided datasheets, as a function of the reading (RD) or of the full-scale (FS).

Uncertainties in the experimental measurements were calculated according to error propagation analysis [37–39]. The in-cylinder pressure measurement uncertainty was equal to 0.030 bar; air mass flow uncertainty was equal to 0.054 kg/h; syngas mass flow uncertainty was equal to 0.006 kg/h; natural gas mass flow uncertainty is equal to 0.011 kg/h.

To provide a comprehensive overview of the experimental set-up, the following information, monitored during the experimental campaign, are reported as average reference values: environmental air temperature, 27.5 °C; oil temperature, 90 °C; cooling water temperature, 65 °C.

2.2. Experimental Methodology

The experimental campaign was performed in order to investigate the effect of spark advance (ADV) and natural gas substitution with syngas on combustion and pollutant emissions. Natural gas substitution with syngas has been described through the quantification of the syngas energy share (SES). This term indicates the amount of primary energy supplied by syngas as a substitute of natural gas, and it is expressed by the following:

$$SES = 100 * \frac{\dot{m}_{Syn} \cdot LHV_{Syn}}{\dot{m}_{Syn} \cdot LHV_{Syn} + \dot{m}_{NG} \cdot LHV_{NG}} \quad (1)$$

To evaluate effects of ADV and SES on combustion and pollutant characteristics, 12 operating points were chosen, as shown in Table 5. During the experimental phase, the engine was set under the partial (60% of the full load) output load condition. Syngas substitution was realized to provide three different SES levels: 25%, 50%, and 75%. Four different spark advance conditions were tested: 10°, 25°, 35°, and 45° BTDC. The engine rotational speed was fixed to 1500 RPM. This value was chosen in order to replicate a power generation unit, the engine rotational speed fixed to the typical four-poles synchronous generator speed.

The experimental procedure was set-up in order to minimize data dispersions and to provide reliable results. Hence, the engine was stabilized to each operating point and data were acquired only after reaching stability, which was done by keeping the engine in stable conditions for a sampling time equal to 4 min. Emission measurements were performed with a sampling rate of 1Hz and were averaged based on the sampling time. The mean in-cylinder pressure trace calculation, which will be described in the following section, was obtained by averaging 100 consecutive cycles for each operating point. Repeatability is ensured: a maximum percentage deviation equals 4% in the worst case, and an average deviation below 2% for each of the presented results were calculated.

Table 5. Definition of the 12 operating points based on their: label, SES, and spark advance.

Label	SES [%]	Spark Advance [°BTDC]
OP2510	25	10
OP2525	25	25
OP2535	25	35
OP2545	25	45
OP5010	50	10
OP5025	50	25
OP5035	50	35
OP5045	50	45
OP7510	75	10
OP7525	75	25
OP7535	75	35
OP7545	75	45

2.3. Combustion Analysis

The main aim of the in-cylinder thermodynamic combustion analysis is the evaluation of the pressure evolution and the calculation of in-cylinder temperatures and the rate of heat release, which are fundamental parameters describing combustion characteristics thus presenting the basis for the evaluation of emission formation phenomena. The starting points for 0D thermodynamic analysis are the collection of operating points specific data, such as air and fuel mass flows, and geometrical characteristics of the engine, followed by the in-cylinder pressure data acquisition. The mean in-cylinder pressure trace was calculated by averaging 100 consecutive cycles of the individual operating points, as averaging significantly eliminates point to point variations due to signal noise [40]. A low pass finite impulse response (FIR) filter was applied to the average pressure trace in order to eliminate pressure oscillations in the combustion chamber [41]. A 0D thermodynamic analysis was performed via the "BURN" functionality of the "AVL BOOST" software. The in-cylinder heat transfer was calculated using the "AVL 2000" model, which is a modification of the well-known Woschni heat exchange model, which is able to take into account the effect of heat exchange on the volumetric efficiency [42]. The piston motion and blow-by characteristics were modeled according to "AVL BOOST" [42]; in particular, the piston motion was described using the standard crank train theory, while the blow-by mass flow rates were calculated using the specified effective blow-by gap and the mean crankcase pressure [42].

3. Results and Discussion

3.1. Combustion and Performance Characteristics

The combustion characteristics will be described and discussed based on the experimental analysis that has been carried out. The variations of the spark advance have a direct effect on the fuel combustion propagation, and consequently, on the in-cylinder pressure development. Earlier ignition timings lead to earlier start of combustion and pressure increase, which results in a high-pressure peak that takes place earlier in the expansion stroke [43]. Conversely, retarding the spark advance results in a retarded pressure increase with a lower pressure peak that occurs later in the expansion stroke. This is confirmed by the pressure trends measured at every operating condition. As shown in Figure 2, as the ignition timing advances, the pressure peaks rise substantially. Figure 2 shows the in-cylinder pressure developments at different spark advances, measured with a syngas energy share of 75%. The maximum measured pressure peaks are 14.5 bar, 24.8 bar, 30.5 bar, and 34.5 bar with a spark advance of 10°, 25°, 35°, and 45° BTDC, respectively. Similar increasing values of in-cylinder pressure peaks are measured with SES values equal to 25% and 50%. The maximum measured pressure peaks measured with a SES of 25% are 13.6 bar, 24.0 bar, 29.0 bar, and 32.5 bar with a spark advance of 10°, 25°, 35°, and 45° BTDC, respectively. Finally, with the SES equal to 50%, pressure peaks are 13.4 bar, 23.8 bar, 28.9 bar, and 31.4 bar with a spark advance of 10°, 25°, 35°, and 45° BTDC, respectively.

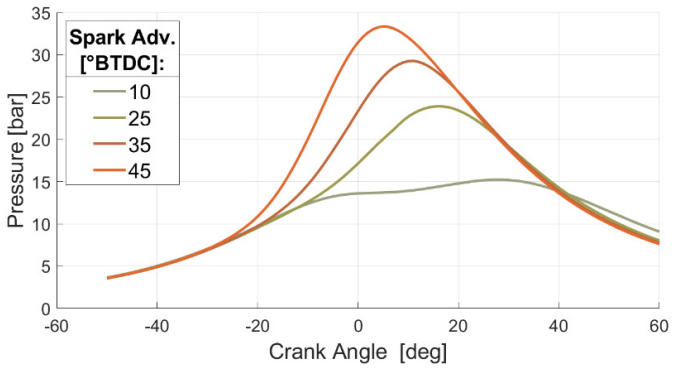

Figure 2. In-cylinder pressure developments for each spark advance (SES: 75%).

As a consequence, IMEP values increased with advancing spark timing values, reaching peak values close to 5 bar. IMEP values are shown in Table 6.

Table 6. IMEP [Bar] values for different spark advance and syngas energy share.

Spark Advance [°BTDC]	IMEP [Bar] @SES: 25%	IMEP [Bar] @SES: 50%	IMEP [Bar] @SES: 75%
10	3.4	3.5	3.9
25	4.1	3.9	4.2
35	4.4	4.4	4.4
45	4.6	4.8	4.7

The different types of mixtures show different combustion behavior under specific conditions. When late combustion strategies are applied, whenever the spark advance values are equal to 25° and 10° BTDC, in-cylinder pressure trends reveal relevant differences with respect to the type of fuel. As shown in Figure 3, while high spark advances pressure trends behave similarly, the different combustion reaction rates at low spark advances affect the in-cylinder pressure. In particular, with a spark advance equal to 10° BTDC, the maximum pressure peaks are obtained when the SES is equal to 75%. Pressure trends rise with increasing SES; however, such behavior is less pronounced at advanced ignition times. Pressure trace levels can be explained by considering the reduction of the charge energy density (CED) as the SES is increased and the increase in the intake manifold pressure as a

result of the decrease in CED to maintain constant torque values. Due to an increased intake manifold pressure when the SES is increased, the pressure traces in Figure 3 coherently show different levels during the compression phase. Different numerical and experimental studies have shown that the laminar flame velocity of a CNG-based mixture tends to increase with an increase of hydrogen fractions [25,44–46]. Indeed, the presence of H_2 in the mixture increases the concentrations of H, O, and OH radicals thus increasing the mixture's overall reaction rate [45–48]. In the case of the syngas enriched CNG, the assessment of the change in laminar flame velocity is more complex. In fact, the effect of N_2 and CO_2 dilution on the rate of reaction of CH_4/H_2 mixtures depends on the specific mixture composition. Several experimental results [49–52] show that laminar flame velocity is reduced with the increase of the dilution ratio because of the lowering of the adiabatic flame temperature of the mixture [25,52,53]. As such, the overall mixture combustion characteristics have to be considered according to the view of the specific operating conditions, such as the spark advance. If we refer to the typical combustion mechanism for spark ignition engines, under late ignition strategy, the temperature and pressure would be initially relatively low, causing a negative effect on the initial flame development and on the following flame propagation process [25]. In these situations, the effect of the presence of the more reactive species in the mixture, such as H_2, is clear when the SES 75% mixture is compared with the SES 50% and SES 25% mixtures and seems to prevail in the countereffect of the N_2 and CO_2 dilution. As the ignition time advances and more time is available for the combustion to progress, the three mixtures tend to behave similarly, as presented by the pressure trends in Figure 3, with spark advances equal to 35° and 45° BTDC.

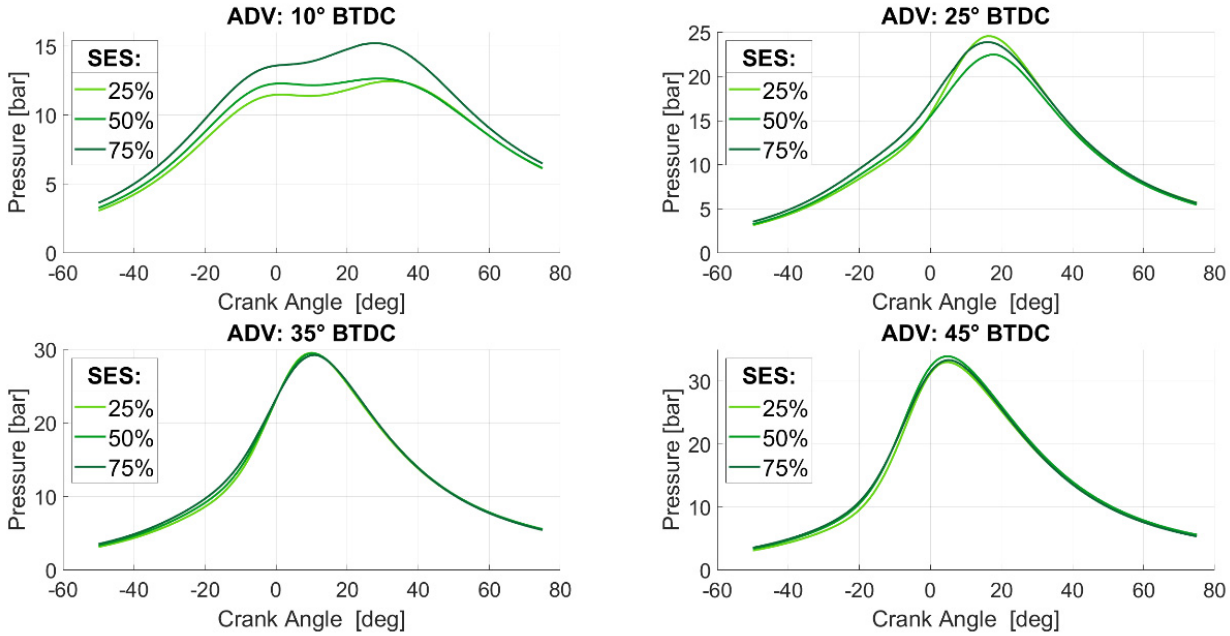

Figure 3. In-cylinder pressure developments for each of the three gas mixtures (SES 25%, 50%, and 75%) at different spark advance (10°, 25°, 35°, and 45° BTDC).

These considerations are enforced by the rate of heat release (ROHR) analysis. As shown in Figure 4, heat release trends reveal different combustion characteristics with fuel mixtures tested at a spark advance equal to 10° BTDC. Combustion development occurs earlier with the high SES mixtures due to the presence of more reactive species (H_2). For earlier spark advances in particular, the combustion duration is shorter due to higher in-cylinder temperatures, which increase laminar flame velocity. As the ignition time advances, the effect of the presence of non-reactive species such as N_2 and CO_2 becomes more visible. In fact, the SES 25% mixture shows the highest values of ROHR. Peaks in ROHR experienced with the SES 25% mixture with spark advances equal to 35° and 45°

BTDC have a percentage increase of 19% and 21%, respectively, with respect to the SES 75% mixture. This can be clearly attributed to the high dilution ratio of the syngas-rich mixtures [49–51], which consequently also have a relevant effect in decreasing the mixture combustion temperature.

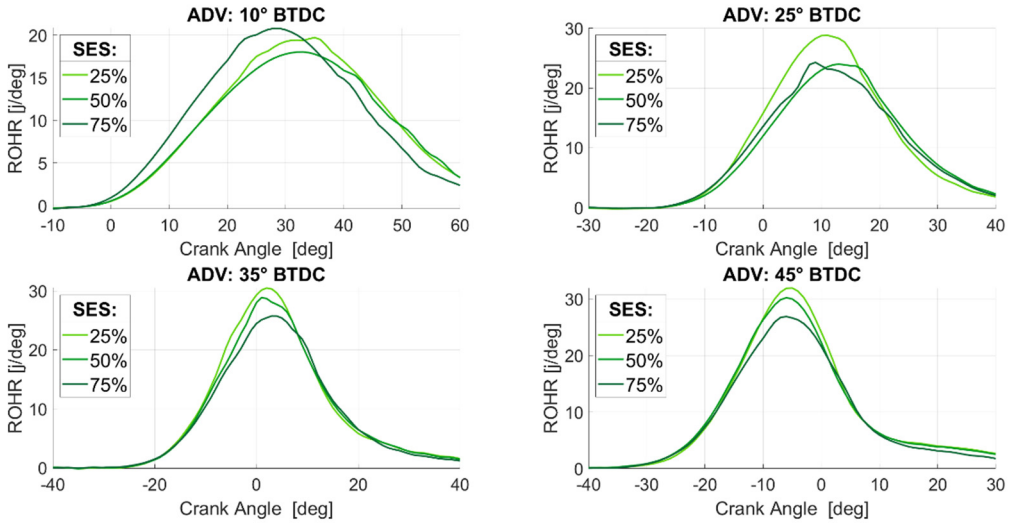

Figure 4. ROHR developments for each of the three gas mixtures (SES 25%, 50%, and 75%) at different spark advances (10°, 25°, 35°, and 45° BTDC).

Brake thermal efficiency (BTE) and output torque results are shown in Figure 5. As clearly seen from the bar plot, BTE is strongly influenced by the spark advance rather than the syngas energy share. The lowest spark advance corresponds to the lowest BTE, and this is confirmed for each of the SES. Instead, operating points with a spark advance equal to 35°BTDC show the best performance, reaching BTE values close to 28%.

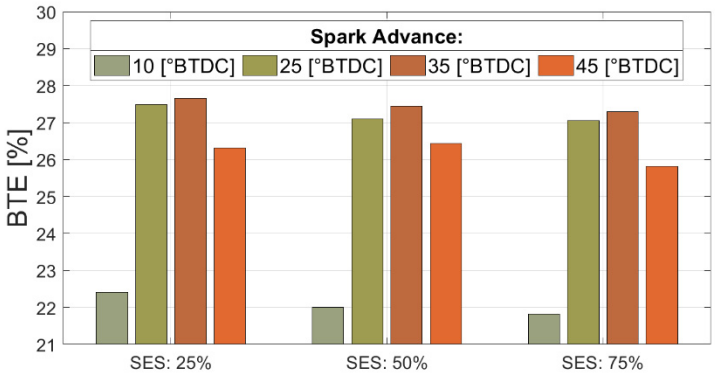

Figure 5. Brake thermal efficiency power for different spark advance and syngas energy share.

The increasing in-cylinder pressure, a consequence of the advancing spark timing, tends to boost the output torque. As shown in Table 7, the output average torque increases with the ignition time; it reaches a maximum, and then it decrease for all of the investigated SES levels. In fact, the higher pressures promote an increase of net work, but, at the same time, when the ignition time increases too much, the increasing pressure in the compression phase leads to negative torque and an increased heat transfer rate due to higher in-cylinder temperatures that result in lower pressure in the expansion phase, so the output torque starts to decrease. Peak output torque is measured at the spark advance equal to 25° BTDC for SES 25%, while for both SES 50% and 75%, peak output torque is measured at the spark 35° BTDC.

Table 7. Torque [Nm] values for different spark advances and syngas energy share.

Spark Advance [°BTDC]	Torque [Nm] @SES: 25%	Torque [Nm] @SES: 50%	Torque [Nm] @SES: 75%
10	55.5	54.1	53.5
25	68.0	66.6	65.3
35	67.1	67.0	66.7
45	65.0	64.4	64.1

A further consideration can be made with respect to the power derating caused by the use of syngas. Figure 6 shows how the increasing amount of syngas in the mixtures brings a decrease in output power in the range of 2–6%. Such behavior is commonly attributed to the decrease in the calorific value of the air-fuel mixture; comparable power derating values can be found in the literature [30].

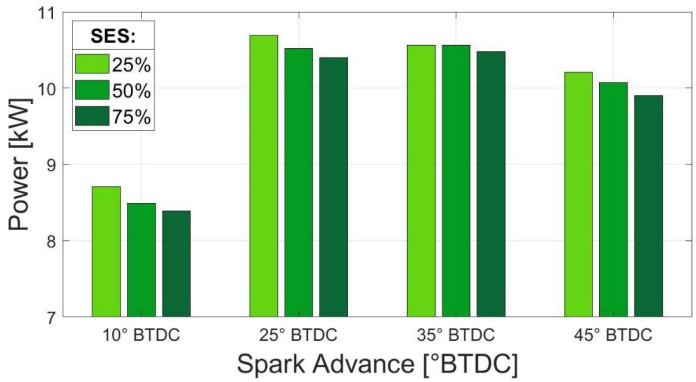

Figure 6. Output power for different spark advance and syngas energy share.

As a result of the discussion on combustion and performance characteristics, two of the three research questions can now be properly answered. In particular, how (i) the BTE vary as a consequence of the different fueling strategies, and how (ii) the power derating is effectively representing a limiting factor have been quantified. The impact of the different fuel mixtures on BTE is negligible if compared to the spark advance variation ones. Such findings could help in the definition of an optimization strategy that considers spark advance control as a primary control variable for optimal BTE. On the other hand, power derating is confirmed for every timing strategy, but it is minimized at 35° BTDC—namely when BTE is maximized. This finding suggests the definition of a possible fueling optimization strategy in which BTE maximization and power derating minimization can be reached at the same time.

3.2. Emission Characteristics

Pollutant emissions have been measured and analyzed in terms of the presence of NO_x, CO, THC, and CO_2 in the exhaust gasses. The measured values are reported in Figures 7 and 8. Emissions of NO_x are correlated to a number of different chemo–physical interactions between the fuel and air as well as to the specific operative conditions. Several technical and physical parameters such as cylinder pressure, combustion temperature, air-fuel ratio, combustion duration, humidity, and the possible oxygen content of the fuel [54–56] are involved.

3.2.1. NO_x Emissions

From the analysis of NO_x emissions, it has emerged how the two independent variables (SES and spark advance) act differently and often in opposition to each other. The competing effects should be addressed and explained.

First, the effect of spark advance on NO_x emissions is discussed. The main NO_x formation paths are identified in the presence of oxygen in the fuel as well as in high

combustion temperatures and pressures reached during the combustion process [43]. As shown in Figure 7, a general increase of NO_x emissions is clear as the spark advance values advance. Such behavior can be clearly attributed to the increase of the combustion temperature created by the earlier start of ignition. This is confirmed by the in-cylinder pressure (Figure 3) and the ROHR (Figure 4) trends. Moreover, as the natural gas fraction of the mixture decreases, the increasing trends of NO_x emissions with the spark advance is less evident. Comparing the results obtained with minimum (10° BTDC) and maximum (45° BTDC) spark advances, when the SES is equal to 25%, the growth in NO_x emissions due to the effect of the spark advance is equal to 75%. Similarly, when the SES is equal to 50% or 75%, the increase in NO_x emissions due to the effect of the spark advance is equal to 60% or 20%, respectively. When the engine runs with a spark advance equal to 45° BTDC, which represents the most critical condition, the maximum NO_x emissions are measured in roughly 1600 ppm (SES 25%) and reach a minimum value of roughly 500 ppm (SES 75%).

The effect of the second independent variable, namely the syngas energy share, on NO_x emissions will be now taken into consideration. In order to correctly assess the emission characteristics, the mixture composition should be discussed. Whenever NG and syngas are blended, the gas composition strongly influences the combustion temperature, and consequently, the emissions. The competing effects should be taken into account. On one hand, H_2 and CO in syngas increase the combustion temperature that facilitates the thermal formation of NO_x [27]. Moreover, the relative amounts of CO and H_2 can also have a significant impact on NO_x emissions, as stated by Hasegawa et al. [57]: the higher the CO/ H_2 molar ratio, the slower the O_2 consumption rate; higher concentrations of O_2 are available for NO_x formation, and as a result, the NO_x production rate is increased [57]. On the other hand, the presence of CO_2 and N_2 tends to strongly decrease the combustion temperature, which also decreases the NO_x formation [58]. As a result of the experimental campaign, it can be concluded that, under the tested conditions, the second of the two competing effects is prevaling, as NO_x emissions reduce with increasing SES (Figure 7).

To summarize the main findings, it can be stated that as a consequence of the advancing spark timing, the rate of NO_x formation reactions increases. On the contrary, increasing syngas energy shares promote a decrease inthe rates of NO_x formation reactions due to the growing amount of CO_2 and N_2 in the fuel mixture; hence, the countereffect of the growing presence of CO and H_2, which is demonstrated to be responsible for higher rates of NO_x formation [57], is substantially hindered.

3.2.2. CO Emissions

A general increase of CO emissions is correlated to the increasing share of syngas in the fuel mixture (Figure 7). Minimum values of CO are measured with SES equal to 25% (from 0.10 to 0.17 %vol), while maximum CO emissions are reached with SES equal to 75% (from 0.22 to 0.27 %vol). These results can be explained considering two main paths, both dealing with the syngas composition. While syngas is composed of different species, each one with different physio-chemical characteristics, natural gas, due to its simpler composition and very low share of inert gases, mixes more homogeneously with air, which results in a more efficient burning process [27,59]. When syngas is added to the mixture, less efficient mixing of different species might create regions with equivalence ratios outside the flammability limits, in particular, in colder regions, which promotes the formation of CO [60]. Moreover, when discussing CO emissions from syngas combustion, a second path is usually considered: a relevant share of CO in the exhaust gases originates from the incomplete combustion of the hydrocarbon species in the syngas itself [59,60]. Advanced spark advance values produce a small increase in CO emissions. This tendency is confirmed for each of the three SES conditions. This behavior can be correlated to the mechanism of formation for CO.

3.2.3. THC Emissions

When a complex mixture of different gases is used as a fuel in a spark ignition engine, the oxidation of hydrocarbons occurs when the proper conditions for temperature, pressure, and radical species formation coexist. Hence, residence time plays a fundamental role. As shown in Figure 4, for high ignition advance, heat is released in a shorter time-span, and a significant amount of it is released before TDC: such heat gradients reveal a shorter residence time at adequate conditions for the oxidation of hydrocarbons [27,60], which is reflected in THC emissions. As shown in Figure 7, THC emissions increase when the spark is advanced, while they decrease when the syngas share in the mixture increases. In particular, when the SES equals 25%, the late-to-early ignition variation boosts the THC emissions from roughly 125 ppm to 300 ppm. Similarly, when the SES equals 50% or 75%, THC emissions rise from roughly 80 ppm to 173 ppm or from roughly 60 ppm to 132 ppm, respectively. The decreasing values of THC with increasing SES can be attributed to the increased H_2 content in the fuel mixture, which is responsible for promoting fast conversion of hydrocarbons [27,61].

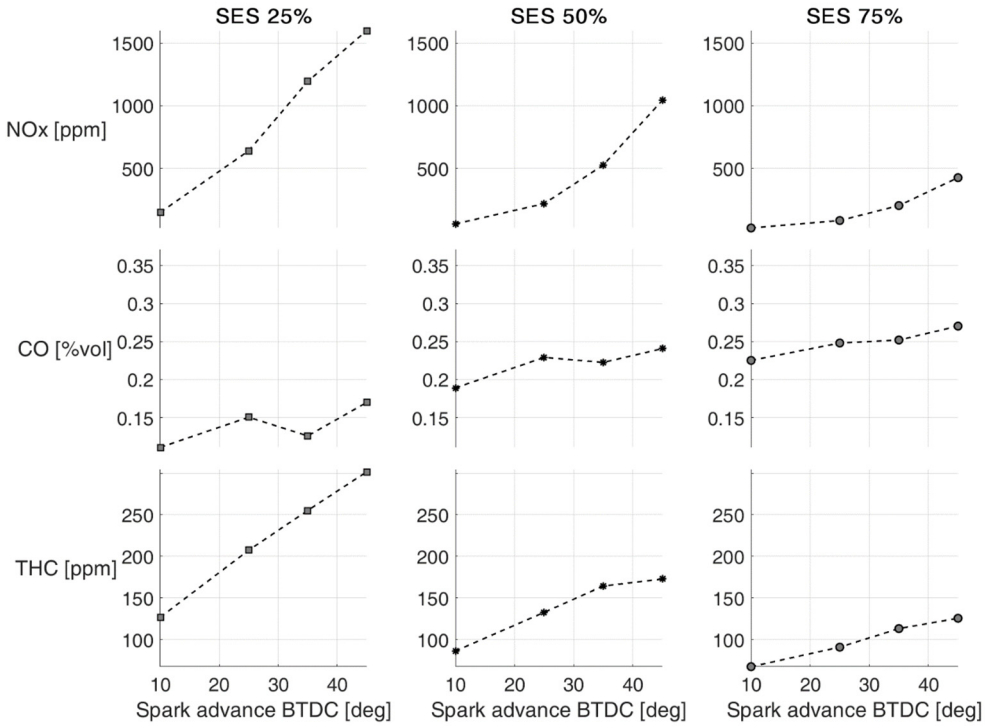

Figure 7. NO_x [ppm], CO [%vol], and THC [ppm] emissions for different spark advances and syngas energy share.

3.2.4. CO_2 Emissions

An increase in the CO_2 emissions is observed when using high syngas energy shares in the fuel mixture. As shown in Figure 8, a constant increase of CO_2 emissions is determined when the SES is increased: values in the range of 10.0%, 12.0%, and 13.8% CO_2 in the exhaust are measured with the SES equal to 25%, 50%, and 75%, respectively. The increase in the CO_2 concentration in the exhaust is usually attributed to two main reasons: the presence of CO_2 in the syngas and the conversion of CO [62]. Results show how the influence of spark advances on CO_2 emissions is negligible with respect to the changing gas composition. This clearly suggests that the increase of CO_2 has a primary path, whichis the presence of CO_2 in the mixture.

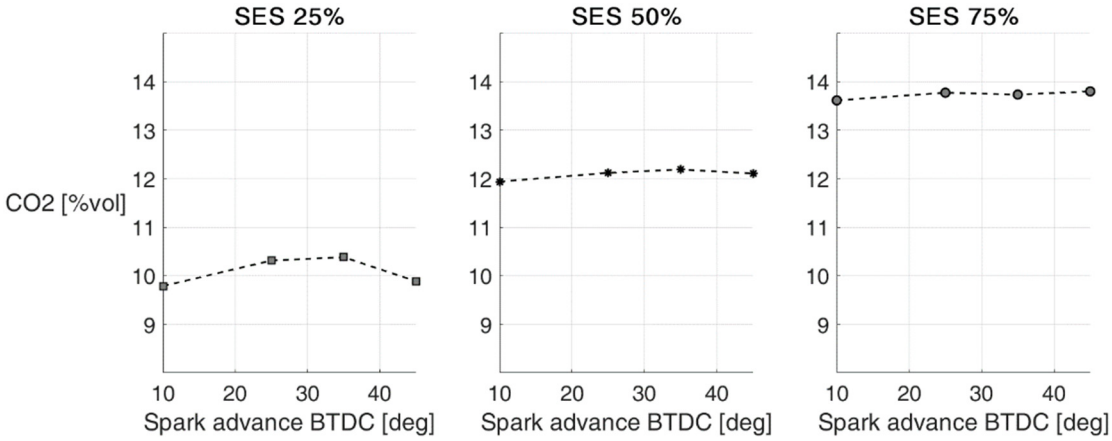

Figure 8. CO_2 [%vol] emissions for different spark advance and syngas energy share.

Finally, to be consistent with the European directives in terms of pollutant emissions mitigation in the power generation sector [63], the emission results have been reported in g/kWh in Table 8 together with the operating points' brake power output [kW] indication. In accordance with the data presented in Table 8, some interesting observations can be obtained. When comparing operating points with the spark advance equal to 35° BTDC (namely labeled OP2535, OP5035, and OP7535), which is the one ensuring the highest BTE, a remarkable drop in NO_x emissions is measured (from 6.59 to 1.31 g/kWh) when the SES increases from 25% to 75%. On the other hand, under the same conditions, an increase in CO_2 emission is measured (from 84.15 to 130.21 g/kWh). However, since the tested syngas replicates a typical forestry biomass producer gas composition, the increase in the SES would also create a growing share of bio-based fuel, emitted CO_2 of which can be considered as a net-zero CO_2 [63]. Hence, the NO_x—CO_2 emissions tradeoff has to be occurred, taking into consideration the type of fuel primary sources and its origin.

Table 8. Emissions [g/kWh] and brake power [kW] for each of the operating points according to its label (OPXXYY: OP = Operating Point, XX = SES, YY = spark advance; see Table 5).

Label	Brake Power [kW]	CO [g/kWh]	CO_2 [g/kWh]	NO_x [g/kWh]	THC [g/kWh]
OP2510	8.72	0.70	96.97	1.00	0.37
OP2525	10.68	0.77	83.07	3.51	0.49
OP2535	10.54	0.65	84.15	6.59	0.61
OP2545	10.21	0.91	83.67	9.23	0.75
OP5010	8.50	1.31	129.65	0.41	0.28
OP5025	10.46	1.28	106.66	1.30	0.34
OP5035	10.52	1.24	106.34	3.12	0.42
OP5045	10.12	1.41	111.42	6.54	0.47
OP7510	8.40	1.70	161.32	0.19	0.24
OP7525	10.26	1.53	133.23	0.54	0.26
OP7535	10.48	1.52	130.21	1.31	0.32
OP7545	10.07	1.69	135.60	2.85	0.36

On the basis of the analysis and discussion of the emission results, the third research question can be now answered. It is now clear how pollutant emission (NO_x, CO, THC, CO_2) formation is affected by the use of different fueling strategies, and in particular, how the two independent variables (SES and spark advance) act differently, and often in opposition, has emerged. For example, the rate of NO_x formation reactions is increased whenever the combustion strategy favors an earlier start of ignition (advancing values of the spark advance); on the contrary, rates of NO_x formation reactions are decreased when the fueling strategy favors a growing amount of CO_2 and N_2 in the fuel mixture (increasing values of the SES). Similarly, inhomogeneous mixtures (increasing values of the SES) lead to an increase in CO emissions while THC emissions decrease (due to increasing values of H_2). Such findings underline how an optimization strategy aimed at reducing

pollutant emissions should be based on complex and conflicting interactions. Only an integrated approach able to consider the formation of all of the main pollutant species at the same time could be used effectively as an emission optimization strategy. Moreover, the origin of the primary source used to produce syngas is fundamental to estimate the level of carbon-neutrality of the obtained emissions and should be considered as an organic optimization strategy.

4. Conclusions

In the presented work, a light duty spark-ignition engine operating with natural gas and syngas has been used to characterize the effect of the use of gaseous fuel mixtures on combustion and emissions characteristics. The composition of syngas replicates the typical syngas obtained from biomass gasification, while the natural gas features very high methane share and could be therefore substituted with a biomethane. The use of mixtures of natural gas and biomass-generated syngas is crucial for real applications, where a shortage of primary sources or power derating issues may result in the need to complement syngas with natural gas. Investigations have been carried out considering two main independent variables: the syngas energy share (SES), which represents the amount of primary energy supplied by syngas as a substitute for natural gas, and the spark advance. The performance analysis revealed that the optimal spark timing (35° BTDC) does not change with the energy shares. Complementing syngas with natural gas creates an increase of NO_x and THC, while CO and CO_2 tend to increase with increasing SES. In particular, the most important findings are presented below:

- Brake thermal efficiency (BTE) is strongly influenced by the spark advance more so than by the syngas energy share. The lowest spark advance (10° BTDC) corresponds to the lowest BTE, while the operating points with a spark advance equal to 35° BTDC show the best performance, reaching BTE values close to 28%;
- Increasing the amount of syngas in the mixture creates a decrease in output power in the range of 2–6%. Hence, considering the significantly reduced volumetric energy density of the fuel, only minor power derating is experienced with the use of syngas;
- A general increase of NO_x emissions is associated with advancing values of the spark advance. Such behavior is addressed to the increase of the combustion temperature created by the earlier start of ignition, confirmed by the in-cylinder pressure and ROHR analysis;
- On the other hand, the presence of syngas in the fuel mixture tends to promote a decrease in the rates of NO_x formation reactions due to an increased share of CO_2 and N_2 in the fuel mixture;
- A general increase of CO emissions is correlated to the increasing share of syngas in the fuel mixture. The less efficient mixing of the different species might create regions with equivalence ratios outside the flammability limits, in particular, in colder regions and promotes the formation of CO. Moreover, a relevant share of CO in the exhaust gases originates from the incomplete combustion of CO already present in the syngas itself;
- THC emissions increase with advancing spark timing, while they decrease when the syngas share in the mixture increases. This can be attributed to the increased H_2 content in the fuel mixture, which is responsible for promoting fast conversion of hydrocarbons;
- Increases in the CO_2 emissions are measured as the syngas energy share in the fuel mixture increases, while the influence of spark advance on CO_2 emissions is negligible with respect to the changes in gas composition. This clearly suggests how the increase of CO_2 has a primary path, which is the presence of CO_2 in the fuel mixture. However, part of this growing amount of CO_2 should be considered in light of the type of syngas primary source, the bio-based origin of which is responsible for net-zero emissions.

The main quantitative findings of the article as well as the experimental methodology presents a practical basis for further optimization procedures. Through the latter, different

goals could be simultaneously achieved, such as (i) increasing engine effective efficiency, (ii) mitigating engine emissions, and (iii) ensuring constant engine power, which is crucial in different real-world applications. Further steps in the presented research work could be represented by the development and the application of an experimental data driven optimization strategy.

Author Contributions: Conceptualization, C.C., U.Ž.B., M.R., T.S., S.R.O. and T.K.; data curation, C.C.; formal analysis, C.C., U.Ž.B., T.S. and S.R.O.; investigation, C.C., U.Ž.B., M.R., T.S. and S.R.O.; methodology, C.C., U.Ž.B., M.R., T.S., S.R.O. and T.K.; project administration, T.K.; resources, T.K.; software, C.C. and U.Ž.B.; supervision, U.Ž.B., M.R., T.S., S.R.O., M.B. and T.K.; visualization, C.C.; writing—original draft, C.C.; writing—review and editing, C.C., U.Ž.B., M.R., T.S., S.R.O., M.B. and T.K. All authors have read and agreed to the published version of the manuscript.

Funding: This research received no external funding.

Institutional Review Board Statement: Not applicable.

Informed Consent Statement: Not applicable.

Data Availability Statement: Not applicable.

Conflicts of Interest: The authors declare no conflict of interest.

References

1. Dhyani, V.; Subramanian, K.A. Experimental based comparative exergy analysis of a multi-cylinder spark ignition engine fuelled with different gaseous (CNG, HCNG, and hydrogen) fuels. *Int. J. Hydrogy Energy* **2019**, *44*, 20440–20451. [CrossRef]
2. Elnajjar, E.; Hamdan, M.O.; Selim, M.Y.E. Experimental investigation of dual engine performance using variable LPG composition fuel. *Renew. Energy* **2013**, *56*, 110–116. [CrossRef]
3. Elnajjar, E.; Selim, M.Y.E.; Hamdan, M.O. Experimental study of dual fuel engine performance using variable LPG composition and engine parameters. *Energy Convers. Manag.* **2013**, *76*, 32–42. [CrossRef]
4. Wróblewski, P.; Iskra, A. *Problems of Reducing Friction Losses of a Piston-Ring-Cylinder Configuration in a Combustion Piston Engine with an Increased Isochoric Pressure Gain*; SAE Technical Paper 2020-01-2227; SAE International: Warrendale, PA, USA, 2020.
5. European Commission. *Communication from the Commission to the European Parliament, the European Council, the Council, the European Economic and Social Committee and the Committee of the Regions*; The European Green Deal. COM/2019/640 Final; European Commission: Brussels, Belgium, 2019.
6. Vakalis, S.; Caligiuri, C.; Moustakas, K.; Malamis, D.; Renzi, M.; Baratieri, M. Modeling the emissions of a dual fuel engine coupled with a biomass gasifier—Supplementing the Wiebe function. *Environ. Sci. Pollut. Res.* **2018**. [CrossRef]
7. Antolini, D.; Brianti, B.; Caligiuri, C.; Borooah, R.; Patuzzi, F.; Baratieri, M. Energy Valorization of Forestry Residues through a Small-Scale Open Top Gasifier. In Proceedings of the Biomass Technologies and Conversion for Bioenergy—28th European Biomass Conference and Exhibition, Virtual, 6–9 July 2020; pp. 407–410.
8. Antolini, D.; Ail, S.S.; Patuzzi, F.; Grigiante, M.; Baratieri, M. Experimental investigations of air-CO_2 biomass gasification in reversed downdraft gasifier. *Fuel* **2019**, *253*, 1473–1481. [CrossRef]
9. Korakianitis, T.; Namasivayam, A.M.; Crookes, R.J. Natural-gas fueled spark-ignition (SI) and compression-ignition (CI) engine performance and emissions. *Prog. Energy Combust. Sci.* **2011**, *37*, 89–112. [CrossRef]
10. Faramawy, S.; Zaki, T.; Sakr, A.A.-E. Natural gas origin, composition, and processing: A review. *J. Nat. Gas Sci. Eng.* **2016**, *34*, 34–54. [CrossRef]
11. Srinivasan, K.K.; Agarwal, A.K.; Krishnan, S.R.; Mulone, V. *Natural Gas Engines—For Transportation and Power Generation*; Springer: Berlin/Heidelberg, Germany, 2019; ISBN 9789811333064.
12. Corbin, J.C.; Peng, W.; Yang, J.; Sommer, D.E.; Trivanovic, U.; Kirchen, P.; Miller, J.W.; Rogak, S.; Cocker, D.R.; Smallwood, G.J.; et al. Characterization of particulate matter emitted by a marine engine operated with liquefied natural gas and diesel fuels. *Atmos. Environ.* **2020**. [CrossRef]
13. Monteiro, E.; Bellenoue, M.; Sottton, J.; Roubo, A. *Syngas Application to Spark Ignition Engine Working Simulations by Use of Rapid Compression Machine*; IntechOpen: London, UK, 2012.
14. European Parliament. Directive (EU) 2018/2001 of the European Parliament and of the Council on the promotion of the use of energy from renewable sources. *Off. J. Eur. Union* **2018**, *2018*, 82–209.
15. FAO Forestry Department. *Wood Gas as Engine Fuel*; FAO: Rome, Italy, 1986.
16. Kaupp, A.; Goss, J.R. *Small Scale Gas Producer-Engine Systems*; Vieweg+Teubner Verlag: Wiesbaden, Germany, 1984; ISBN 978-3-528-02001-9.
17. Hagos, F.Y.; Aziz, A.R.A.; Sulaiman, S.A. Trends of Syngas as a Fuel in Internal Combustion Engines. *Adv. Mech. Eng.* **2014**, *6*, 401587. [CrossRef]

18. Martínez, J.D.; Mahkamov, K.; Andrade, R.V.; Silva Lora, E.E. Syngas production in downdraft biomass gasifiers and its application using internal combustion engines. *Renew. Energy* **2012**, *38*, 1–9. [CrossRef]
19. Martinez-Boggio, S.D.; Merola, S.S.; Teixeira Lacava, P.; Irimescu, A.; Curto-Risso, P.L. Effect of fuel and air dilution on syngas combustion in an optical SI engine. *Energies* **2019**, *12*, 1566. [CrossRef]
20. Rosha, P.; Dhir, A.; Mohapatra, S.K. Influence of gaseous fuel induction on the various engine characteristics of a dual fuel compression ignition engine: A review. *Renew. Sustain. Energy Rev.* **2018**, *82*, 3333–3349. [CrossRef]
21. Sridhar, G.; Sridhar, H.V.; Dasappa, S.; Paul, P.J.; Rajan, N.K.S.; Mukunda, H.S. Development of producer gas engines. *Proc. Inst. Mech. Eng. Part D J. Automob. Eng.* **2005**, *219*, 423–438. [CrossRef]
22. Villarini, M.; Marcantonio, V.; Colantoni, A.; Bocci, E. Sensitivity Analysis of Different Parameters on the Performance of a CHP Internal Combustion Engine System Fed by a Biomass Waste Gasifier. *Energies* **2019**, *12*, 688. [CrossRef]
23. Hagos, F.Y.; Aziz, A.R.A.; Sulaiman, S.A. Methane enrichment of syngas (H_2/CO) in a spark-ignition directinjection engine: Combustion, performance and emissions comparison with syngas and Compressed Natural Gas. *Energy* **2015**, *90*, 2006–2015. [CrossRef]
24. Talibi, M.; Hellier, P.; Ladommatos, N. Combustion and exhaust emission characteristics, and in-cylinder gas composition, of hydrogen enriched biogas mixtures in a diesel engine. *Energy* **2017**, *124*, 397–412. [CrossRef]
25. Yan, F.; Xu, L.; Wang, Y. Application of hydrogen enriched natural gas in spark ignition IC engines: From fundamental fuel properties to engine performances and emissions. *Renew. Sustain. Energy Rev.* **2018**, *82*, 1457–1488. [CrossRef]
26. Hagos, F.Y.; Aziz, A.R.A.; Sulaiman, S.A.; Mamat, R. Effect of fuel injection timing of hydrogen rich syngas augmented with methane in direct-injection spark-ignition engine. *Int. J. Hydrogy Energy* **2017**, *42*, 23846–23855. [CrossRef]
27. Nadaleti, W.C.; Przybyla, G. SI engine assessment using biogas, natural gas and syngas with different content of hydrogen for application in Brazilian rice industries: Efficiency and pollutant emissions. *Int. J. Hydrogy Energy* **2018**, *43*, 10141–10154. [CrossRef]
28. Cameretti, M.C.; Cappiello, A.; De Robbio, R.; Tuccillo, R. Comparison between Hydrogen and Syngas Fuels in an Integrated Micro Gas Turbine/Solar Field with Storage. *Energies* **2020**, *13*, 4764. [CrossRef]
29. Elnajjar, E.; Selim, M.; Omar, F. Comparison Study of Dual Fuel Engine Performance and Overall Generated Noise under Different Dual Fuel Types and Engine Parameters. *Int. J. Basic Appl. Sci. IJBAS-IJENS* **2011**, *11*.
30. Nadaleti, W.C.; Przybyla, G. Emissions and performance of a spark-ignition gas engine generator operating with hydrogen-rich syngas, methane and biogas blends for application in southern Brazilian rice industries. *Energy* **2018**, *154*, 38–51. [CrossRef]
31. Kan, X.; Zhou, D.; Yang, W.; Zhai, X.; Wang, C.-H. An investigation on utilization of biogas and syngas produced from biomass waste in premixed spark ignition engine. *Appl. Energy* **2018**, *212*, 210–222. [CrossRef]
32. Bates, R.; Dölle, K. Syngas Use in Internal Combustion Engines—A Review. *Adv. Res.* **2017**, *10*, 1–8. [CrossRef]
33. Soria, J.; Li, R.; Flamant, G.; Mazza, G.D. Influence of pellet size on product yields and syngas composition during solar-driven high temperature fast pyrolysis of biomass. *J. Anal. Appl. Pyrolysis* **2019**. [CrossRef]
34. Lin, C.L.; Weng, W.C. Effects of different operating parameters on the syngas composition in a two-stage gasification process. *Renew. Energy* **2017**. [CrossRef]
35. Danardono, D.; Kim, K.S.; Lee, S.Y.; Lee, J.H. Optimization the design of venturi gas mixer for syngas engine using three-dimensional CFD modeling. *J. Mech. Sci. Technol.* **2011**, *25*, 2285–2296. [CrossRef]
36. Horiba, L. *On Board Emission Measurement System OBS-2200—Instruction Manual*; Horiba Europe GmbH: Oberursel, Germany, 2007.
37. Žvar Baškovič, U.; Vihar, R.; Seljak, T.; Katrašnik, T. Feasibility analysis of 100% tire pyrolysis oil in a common rail Diesel engine. *Energy* **2017**, *137*, 980–990. [CrossRef]
38. Vihar, R.; Žvar Baškovič, U.; Seljak, T.; Katrašnik, T. Combustion and emission formation phenomena of tire pyrolysis oil in a common rail Diesel engine. *Energy Convers. Manag.* **2017**, *149*, 706–721. [CrossRef]
39. Žvar Baškovič, U. Advanced Combustion Concepts with Innovative Waste Derived Fuels. Ph.D. Thesis, University of Ljubljana, Ljubljana, Slovenia, 2019.
40. Rašić, D.; Vihar, R.; Baškovič, U.Ž.; Katrašnik, T. Methodology for processing pressure traces used as inputs for combustion analyses in diesel engines. *Meas. Sci. Technol.* **2017**. [CrossRef]
41. Žvar Baškovič, U.; Vihar, R.; Mele, I.; Katrašnik, T. A New Method for Simultaneous Determination of the TDC Offset and the Pressure Offset in Fired Cylinders of an Internal Combustion Engine. *Energies* **2017**, *10*, 143. [CrossRef]
42. AVL LIST GmbH. *BOOST—Theory (v2014.1)*; AVL List GmbH: Graz, Austria, 2014.
43. Heywood, J.B. *Internal Combustion Engine Fundamentals*; McGraw-Hill Education: New York, NY, USA, 2018; ISBN 007028637X.
44. Boushaki, T.; Dhué, Y.; Selle, L.; Ferret, B.; Poinsot, T. Effects of hydrogen and steam addition on laminar burning velocity of methane-air premixed flame: Experimental and numerical analysis. *Int. J. Hydrogy Energy* **2012**. [CrossRef]
45. Hu, E.; Huang, Z.; He, J.; Jin, C.; Zheng, J. Experimental and numerical study on laminar burning characteristics of premixed methane-hydrogen-air flames. *Int. J. Hydrogy Energy* **2009**. [CrossRef]
46. Di Sarli, V.; Benedetto, A. Di Laminar burning velocity of hydrogen–methane/air premixed flames. *Int. J. Hydrogy Energy* **2007**, *32*, 637–646. [CrossRef]
47. Hu, E.; Huang, Z.; Zheng, J.; Li, Q.; He, J. Numerical study on laminar burning velocity and NO formation of premixed methane-hydrogen-air flames. *Int. J. Hydrogy Energy* **2009**. [CrossRef]

48. Hu, G.; Zhang, S.; Li, Q.F.; Pan, X.B.; Liao, S.Y.; Wang, H.Q.; Yang, C.; Wei, S. Experimental investigation on the effects of hydrogen addition on thermal characteristics of methane/air premixed flames. *Fuel* **2014**. [CrossRef]
49. Coppens, F.H.V.; De Ruyck, J.; Konnov, A.A. The effects of composition on burning velocity and nitric oxide formation in laminar premixed flames of $CH_4 + H_2 + O_2 + N_2$. *Combust. Flame* **2007**. [CrossRef]
50. Miao, H.; Ji, M.; Jiao, Q.; Huang, Q.; Huang, Z. Laminar burning velocity and Markstein length of nitrogen diluted natural gas/hydrogen/air mixtures at normal, reduced and elevated pressures. *Int. J. Hydrogy Energy* **2009**. [CrossRef]
51. Hermanns, R.T.E.; Konnov, A.A.; Bastiaans, R.J.M.; de Goey, L.P.H.; Lucka, K.; Köhne, H. Effects of temperature and composition on the laminar burning velocity of $CH_4 + H_2 + O_2 + N_2$ flames. *Fuel* **2010**. [CrossRef]
52. Salzano, E.; Basco, A.; Cammarota, F.; Di Sarli, V.; Di Benedetto, A. Explosions of Syngas/CO_2 Mixtures in Oxygen-Enriched Air. *Ind. Eng. Chem. Res.* **2012**, *51*, 7671–7678. [CrossRef]
53. Kim, T. Micro methanol reformer combined with a catalytic combustor for a PEM fuel cell. *Int. J. Hydrogy Energy* **2009**, *34*, 6790–6798. [CrossRef]
54. Mirhashemi, F.S.; Sadrnia, H. NOx emissions of compression ignition engines fueled with various biodiesel blends: A review. *J. Energy Inst.* **2020**, *93*, 129–151. [CrossRef]
55. Singh, Y.; Sharma, A.; Tiwari, S.; Singla, A. Optimization of diesel engine performance and emission parameters employing cassia tora methyl esters-response surface methodology approach. *Energy* **2019**, *168*, 909–918. [CrossRef]
56. Alptekin, E. Emission, injection and combustion characteristics of biodiesel and oxygenated fuel blends in a common rail diesel engine. *Energy* **2017**. [CrossRef]
57. Hasegawa, T.; Sato, M.; Nakata, T. A Study of Combustion Characteristics of Gasified Coal Fuel. *J. Eng. Gas Turbines Power* **2001**, *123*, 22–32. [CrossRef]
58. Lieuwen, T.C.; Yang, V.; Yetter, R. *Synthesis Gas Combustion—Fundamentals and Applications*; CRC Press: Boca Raton, FL, USA, 2010; ISBN 9781420085341.
59. Kravos, A.; Seljak, T.; Rodman Oprešnik, S.; Katrašnik, T. Operational stability of a spark ignition engine fuelled by low H2 content synthesis gas: Thermodynamic analysis of combustion and pollutants formation. *Fuel* **2020**, *261*, 116457. [CrossRef]
60. Whitty, K.J.; Zhang, H.R.; Eddings, E.G. Emissions from Syngas Combustion. *Combust. Sci. Technol.* **2008**, *180*, 1117–1136. [CrossRef]
61. Sahoo, B.B.; Sahoo, N.; Saha, U.K. Effect of H_2:CO ratio in syngas on the performance of a dual fuel diesel engine operation. *Appl. Therm. Eng.* **2012**, *49*, 139–146. [CrossRef]
62. Shah, A.; Srinivasan, R.; To, S.D.F.; Columbus, E.P. Performance and emissions of a spark-ignited engine driven generator on biomass based syngas. *Bioresour. Technol.* **2010**, *101*, 4656–4661. [CrossRef]
63. European Environment Agency. The European environment-state and outlook 2020. In *Knowledge for Transition to a Sustainable Europe*; European Environment Agency: Copenhagen, Denmark, 2020; Volume 60, ISBN 9789294800909.